Journal of Hazardous Materials 196 (2011) 426–430

Contents lists available at SciVerse ScienceDirect

Journal of Hazardous Materials

journal homepage: www.elsevier.com/locate/jhazmat

Short communication

Electrospun nanofibers of Bi-doped TiO_2 with high photocatalytic activity under visible light irradiation

Jie Xu, Wenzhong Wang*, Meng Shang, Erping Gao, Zhijie Zhang, Jia Ren

State Key Laboratory of High Performance Ceramics and Superfine Microstructures, Shanghai Institute of Ceramics, Chinese Academy of Sciences, 1295 Dingxi Road, Shanghai 200050, China

ARTICLE INFO

Article history:
Received 3 June 2011
Received in revised form 25 August 2011
Accepted 4 September 2011
Available online 10 September 2011

Keywords:
Nanofibers
Photocatalysis
TiO_2
Bismuth
Visible light

ABSTRACT

Bi-doped TiO_2 nanofibers with different Bi content were firstly prepared by an electrospinning method. The as-prepared nanofibers were characterized by scanning electron microscopy (SEM), X-ray diffraction (XRD), X-ray photoelectron spectroscopy (XPS), photoluminescence spectra (PL), and UV–vis diffuse reflectance spectroscopy (DRS). The results indicated that Bi^{3+} ions were successfully incorporated into TiO_2 and extended the absorption of TiO_2 into visible light region. The photocatalytic experiments showed that Bi-doped TiO_2 nanofibers exhibited higher activities than sole TiO_2 in the degradation of rhodamine B (RhB) and phenol under visible light irradiation ($\lambda > 420$ nm), and 3% Bi:TiO_2 samples showed the highest photocatalytic activities.

1. Introduction

In view of increasingly serious environmental pollution and energy crisis, photocatalysis, a "green" technology, plays an important role in solar energy conversion and degradation of organic pollutants [1]. As a most promising photocatalyst, TiO_2 possesses many advantages such as suitable redox potentials of conduction band and valence band, chemical inertness, stability against photocorrosion, low cost, and nontoxicity [2]. However, the wide band gap (3.2 eV for anatase) and the low quantum efficiency limit the practical application of TiO_2 photocatalyst [3]. It is well known that doping transitional metal ions is one of the most effective methods for synthesizing visible light active TiO_2 photocatalysts with high photocatalytic activities [4]. Some researchers have reported that the incorporation of Bi into TiO_2 lattice not only widens the absorption range of TiO_2 but also acts as an electron acceptor, which is beneficial to the effective separation of photogenerated electrons and holes, thus facilitating photocatalytic reactions [5,6]. Moreover, it should be noted that the morphology of the photocatalysts is another important factor influencing the photocatalytic efficiencies [7,8]. However, such research is still not satisfying considering the practical application of photocatalysts. More effort is needed to obtain Bi-doped TiO_2 photocatalyst with desirable separability and excellent photoactivity.

Fibrous nanostructures are favorable for industrial applications in environmental remediation. On one hand, conventional film photocatalysts can be fixed and reclaimed easily, but their low surface area decreased the photocatalytic activities. On the other hand, the application of particulate photocatalysts is limited owing to the difficulties in separation, which may re-pollute the treated water. Compared to film and particulate counterparts, nanofibrous photocatalysts not only possess large specific surface area, which allow for their surface active sites to be accessible for reactants more efficiently, but also owe high length-to-diameter aspect ratio, which makes the separation of photocatalyst more easily [9]. Electrospining is an effective, straightforward, and convenient way to fabricate polymer, polymer/inorganic hybrid, and inorganic fibers [10]. The electrospun nanofibrous photocatalysts have been found to exhibit excellent performance in terms of photocatalytic activity and recycling [11]. In this work, for the first time, Bi-doped TiO_2 nanofibers were successfully synthesized by electrospinning. We investigated the effects of Bi doping on photocatalytic activities of as-prepared photocatalysts, and 3% Bi:TiO_2 nanofibers showed the highest photocatalytic activity in the degradation of rhodamine B (RhB) and phenol under visible light irradiation ($\lambda > 420$ nm).

2. Experimental

2.1. Synthesis

All reagents used in our experiments were of analytical purity and were used as received without further purification. Certain

* Corresponding author. Tel.: +86 21 5241 5295; fax: +86 21 5241 3122.
E-mail address: wzwang@mail.sic.ac.cn (W. Wang).

0304-3894/$ – see front matter © 2011 Elsevier B.V. All rights reserved.
doi:10.1016/j.jhazmat.2011.09.010

amounts of $Bi(NO_3)_3{\cdot}5H_2O$ were dissolved in the 1.0 g of *N*,*N*-dimethylformamide (DMF) in a capped bottle, then 1.0 g of absolute ethanol and 1.87 g of $Ti(OC_4H_9)_4$ were added into the mixture (the atomic ratio of Bi:Ti ranged from 1% to 3%). The mixture was stirred for several minutes, and 0.28 g of poly(vinyl pyrrolidone) with a molecular weight of 1.3×10^6 was slowly added. After being stirred for 1 h, the solution was loaded in a syringe. The voltage applied to the needle of the syringe was 15 kV and the distance between the tip of needle and aluminum foil was about 20 cm (The setup for electrospinning showed in Fig. S1). The as-collected fibers were calcined at 500 °C for 3 h in air. The as-synthesized samples were denoted as *x*% $Bi:TiO_2$, where *x* refers to the molar ratio of Bi:Ti. The TiO_2 nanofibers were prepared by the same method as described above without adding of $Bi(NO_3)_3{\cdot}5H_2O$.

2.2. Characterization

The phase and composition of as-prepared samples were recorded by X-ray diffraction (XRD) studies using an X-ray diffractometer (Rigaku, Japan). The morphologies and microstructures were performed on a JEOL JSM-6700F field emission scanning electron microscope (SEM). UV–vis diffuse reflectance spectra (DRS) of the sample were recorded with a UV–vis spectrophotometer (Hitachi U-3010). The chemical states of Bi in TiO_2 were analyzed using the X-ray photoelectron spectroscopy (XPS) attachment of a Microlab310F auger microprobe. The photoluminescence spectra (PL) were obtained on a spectrofluorophotometer (Shimadzu RF-5301PC) with a Xe lamp as the excitation source at room temperature.

2.3. Photocatalytic test

Photocatalytic activities of the Bi-doped TiO_2 nanofibers were evaluated by the degradation of rhodamine B (RhB) and phenol under visible light irradiation of a 500 W Xe lamp with a 420 nm cut-off filter. 0.05 g of the photocatalyst was added into 50 mL of RhB (1×10^{-5} M) or 50 mL of phenol (20 mg L^{-1}). Before illumination, the solution was stirred for 30 min in the dark in order to reach adsorption–desorption equilibrium between organic substrates and the photocatalyst. At given irradiation time intervals, a 4 mL solution was sampled. Then, the absorption UV–vis spectrum of the centrifuged solution was recorded with use of a Hitachi U-3010 UV–vis spectrophotometer. In order to prove the visible light photoresponse in actual photodegradation process, 3 W light emitting diodes (LEDs) with different wavelengths were used to excite as-prepared photocatalysts. The photodegradation was carried out in a 20 mL suspension of phenol (20 mg L^{-1}) with 2% $Bi:TiO_2$ photocatalyst (1 g/L). After 4 h irradiation, the corresponding ratio of final concentration to initial concentration (C/C_0) was recorded.

3. Results and discussion

3.1. Characterization of the photocatalysts

The crystal phases of the different materials were investigated by performing XRD analysis. Fig. 1a shows the XRD patterns of sole TiO_2 and Bi-doped TiO_2 samples with different molar ratio of Bi:Ti, demonstrating that all the samples were composed of anatase TiO_2 (JCPDS No.99-0008) and rutile TiO_2 (JCPDS No.99-0090). The introduction of Bi into TiO_2 caused the broadening of diffraction peaks, suggesting lower crystallization degree of Bi-doped TiO_2 samples than that of sole TiO_2, and inhibited the transformation of TiO_2 from anatase-to-rutile, especially for 1% $Bi:TiO_2$. No diffraction peaks indicative of the Bi species could be observed even at Bi:Ti molar ratio up to 3.0% due to low content of Bi. In order to reveal the presence of Bi and its electronic state, X-ray photoelectron spectroscopy

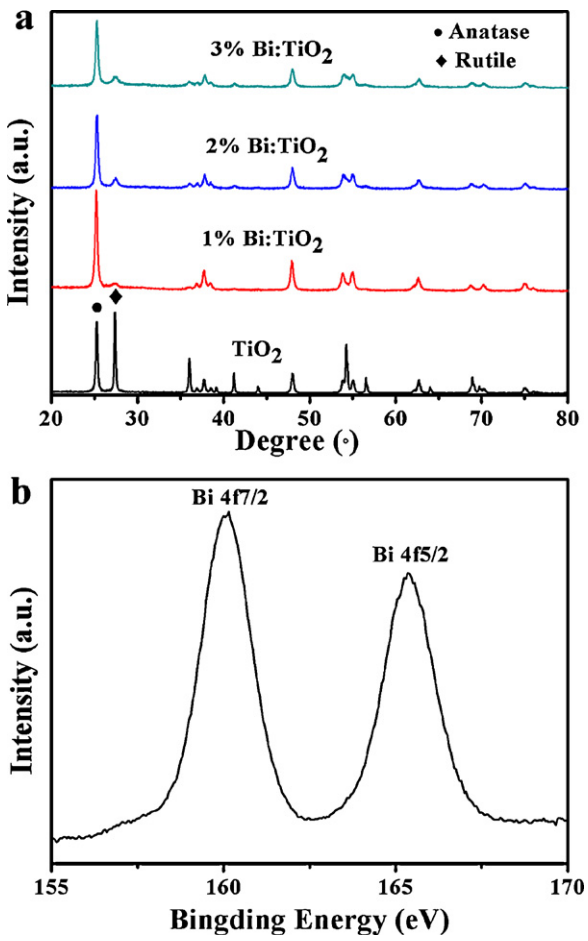

Fig. 1. (a) XRD patterns of TiO_2 and Bi-doped TiO_2 samples and (b) Bi 4f XPS profile of 3% $Bi:TiO_2$ sample.

(XPS) with high resolution is used in our study. Fig. 1b presents the Bi 4f XPS spectra of 3% $Bi:TiO_2$ sample. The peaks of 160.15 eV and 165.35 eV were close to the 4f7/2 level and 4f5/2 level of Bi^{3+} [12], indicating that the incorporated Bi existed in the form of Bi^{3+}.

The morphologies and microstructures of TiO_2 and 3% $Bi:TiO_2$ samples prepared by electrospining are revealed by the SEM images. As shown in Fig. 2a and c, both TiO_2 and 3% $Bi:TiO_2$ exhibited nanofibrous morphologies, and the lengths of these randomly oriented nanofibers could reach several micrometers. The close-up view of TiO_2 nanofibers (Fig. 2b) demonstrated that the diameter of TiO_2 nanofibers ranged from 100 nm to 200 nm, whereas the diameter of 3% $Bi:TiO_2$ nanofibers was between 150 nm and 300 nm as shown in Fig. 2d. It could be observed that the electrospun nanofibers possessed large length-to-diameter aspect ratios, which were beneficial for separation of the photocatalysts from reaction solutions, thus avoiding the possible pollution introduced by unseparated catalysts. In addition, the nanofibers had a rough surface (as shown in Fig. 2b and d) due to the decomposition of PVP during the calcination process, and such rough surface may result in larger surface areas allowing for more efficient contact between reactant molecules and photocatalysts, leading to a higher photocatalytic reaction rate.

The optical absorption property, which is relevant to the electronic structure feature, is considered as a key factor in determining photocatalytic behavior. Fig. 3 presents the UV–vis diffuse reflectance spectroscopy (DRS) of as-prepared samples. Sole TiO_2 displayed no obvious absorbance in visible light region due to its large band gap (3.2 eV for anatase, and 3.0 eV for rutile). All Bi-doped TiO_2 samples exhibited spectral response in the visible region (from

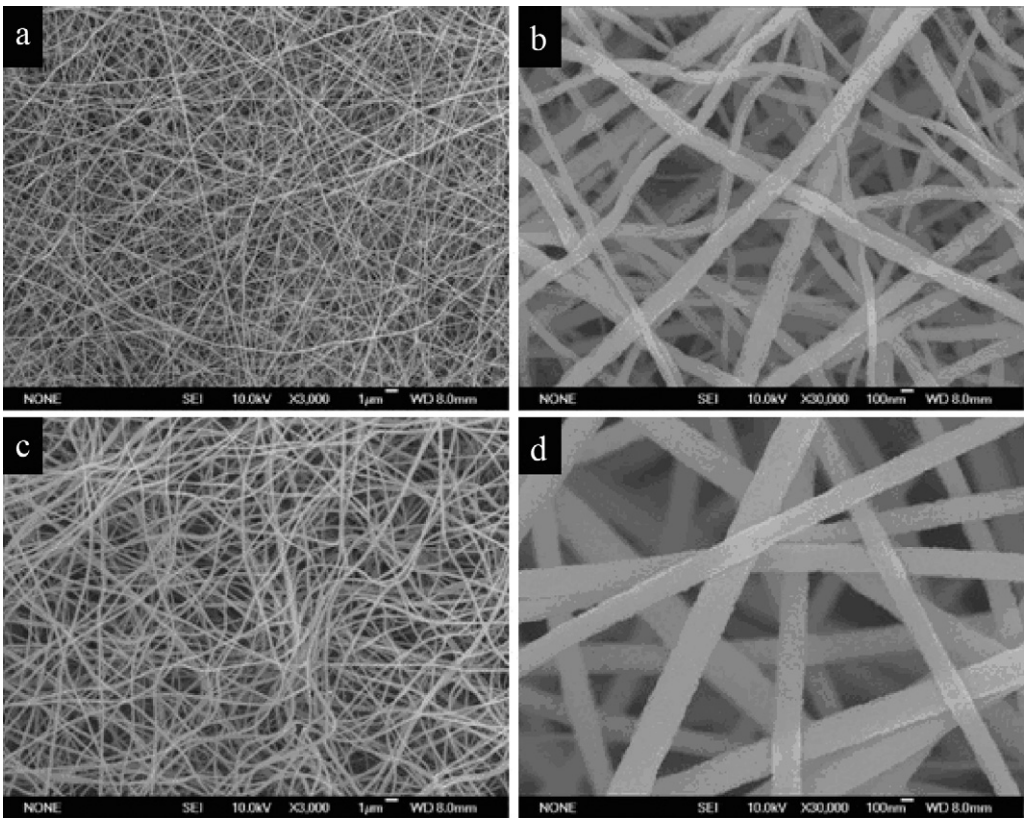

Fig. 2. SEM images of TiO_2 and 3% Bi:TiO_2: (a) low magnification and (b) high magnification of TiO_2; (c) low magnification and (d) high magnification of 3% Bi:TiO_2.

400 nm to 600 nm), and the absorbance became stronger with the increase of Bi content from 0% to 2.0% because of narrower band gap induced by the energy state of Bi^{3+} 6s lone pairs lying above the valence band of sole TiO_2 [13]. However, further increase of Bi content could not enhance the visible absorbance, which was possibly attributed to the lower dispersion of Bi species in TiO_2. In order to prove the effective utilization of absorbed visible light in the photocatalytic process, the photodegradation of phenol was carried out under 3 W LEDs with different wavelengths and Fig. S2 suggests the visible light photoresponse of Bi-doped TiO_2 in the actual photodegradation process.

Photocatalytic activity is closely related to the efficiency of the photogenerated electron–hole separation and the transfer from the inner regions to the outer surfaces. PL emission spectra have been widely used to investigate the efficiency of charge carrier trapping, immigration, transfer, and to understand the fate of photogenerated electrons and holes in the semiconductor [14]. As shown in Fig. 4, TiO_2 and 3% Bi:TiO_2 exhibited emission in the range of 350–550 nm. As for sole TiO_2, the peaks at 435 nm, 449 nm, 451 nm, 467 nm, 491 nm were originated from the surface traps of TiO_2 [15,16]. Compared to sole TiO_2, 3% Bi:TiO_2 exhibited a decrease in the PL intensity, which indicated that 3% Bi:TiO_2 possessed a lower recombination rate of photogenerated electrons and holes. This was possibly ascribed to the fact that Bi species reduced the number of trap states on the surface of TiO_2, thus improved the separation of photogenerated charge carriers [17]. The decreased recombination

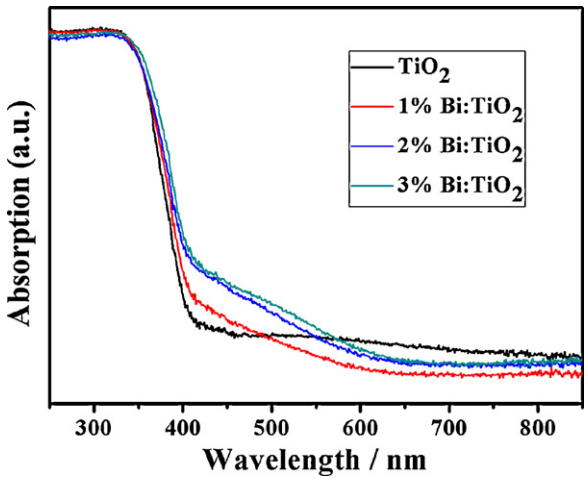

Fig. 3. UV–vis diffuse reflectance spectroscopy (DRS) of sole and Bi-doped TiO_2 samples.

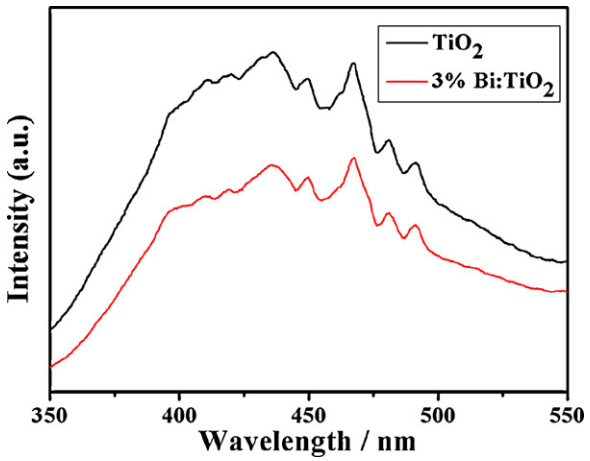

Fig. 4. PL emission spectra of TiO_2 and 3% Bi:TiO_2 samples (excitation wavelength is 300 nm).

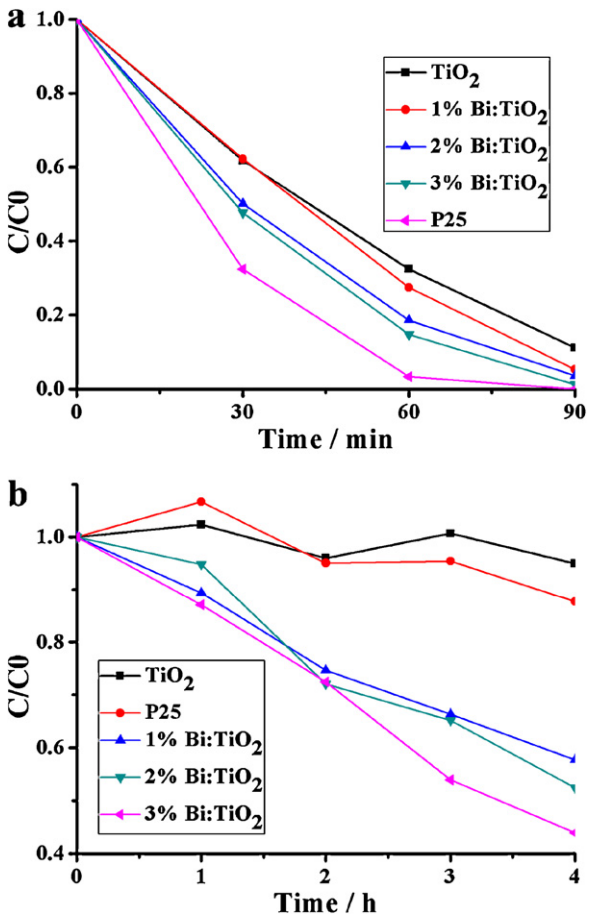

Fig. 5. Photocatalytic degradation profiles of (a) RhB and (b) phenol by TiO_2 and Bi-doped TiO_2 under visible irradiation ($\lambda > 420$ nm).

of photogenerated charges will provide more opportunities for photoinduced charge carriers to participate in the photocatalytic reactions occurring on the semiconductor surface.

3.2. Photocatalytic activity and proposed mechanism

It is well known that the colored rhodamine B (RhB) and uncolored phenol are two kinds of chemicals used in industrial production, which often cause water pollution. Therefore, they are selected as model pollutants to evaluate the photocatalytic activity of the as-prepared TiO_2 samples. Fig. 5a shows the photodegradation of RhB under visible irradiation. Since RhB exhibits absorption band around 553 nm, sole TiO_2 degraded 88.8% of RhB due to the dye sensitization effect [2]. When the Bi:Ti ratio was increased from 0% to 3%, the photocatalytic activities became higher, and RhB was completely degraded in 90 min by 3% Bi:TiO_2. Clearly, doping TiO_2 with Bi^{3+} enhanced the photocatalytic activity, which may be attributed to two reasons. First, the energy band is assumed between the top of the (lone pair) Bi^{3+} 6s band and the bottom of the Ti^{4+} 3d band, giving rise to narrower energy band gap compared to that of TiO_2 [13], which is in accordance with the observation of UV–vis DRS. Hence, the absorption spectra shift into visible light region so that lower energy photons can be absorbed for photocatalytic reaction. Second, Bi species doped in TiO_2 can inhibit the electron and hole recombination by capturing the photoinduced charge carriers as illustrated in PL spectra. Also, P25 (TiO_2), as a well known standard, was used in our work and possessed higher activity for degrading RhB compared to as-prepared samples. On the other hand, Fig. 5b represents the variation of phenol

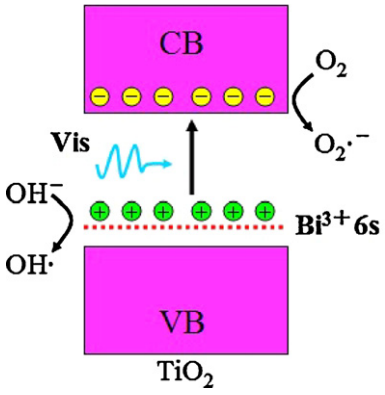

Scheme 1. Proposed mechanism of photocatalytic reaction on Bi-doped TiO_2 photocatalyst.

concentrations (C/C_0) with the irradiation time over TiO_2 and Bi:TiO_2 samples under visible light illumination. Sole TiO_2 degraded very little phenol, only about 5% of phenol in 4 h, which was attributed to the poor ability of TiO_2 in harvesting visible lights. TiO_2 (P25) exhibited very low photocatalytic activity with about 13% of phenol degraded. However, doping TiO_2 with a small amount of Bi species significantly increased the degradation rate, and 3% Bi:TiO_2 showed the highest photocatalytic activity with 56.1% of phenol degraded. In addition, compared to the photodegradation of RhB, the photodegradation of colorless phenol was almost ascribed to the photocatalytic process rather than the dye photosensitization effect.

Based on the above discussions, the level of Bi 6s [8,13,18], which is located above the valence band of TiO_2, plays an important role in reducing the energy band gap of TiO_2, thus enhancing the photocatalytic activity under visible irradiation. Scheme 1 shows the energy band diagram and possible mechanism of photocatalytic reaction on Bi-doped TiO_2, and the detailed photocatalytic processes are proposed as follows (S represents the organic pollutants):

$$\text{Bi} : \text{TiO}_2 \rightarrow \text{Bi}_{6s}(h^+) + \text{TiO}_2(e^-)$$

$$OH^- + h^+ \rightarrow HO^\bullet$$

$$O_2 + e^- \rightarrow O_2^{\bullet -}$$

$$O_2^{\bullet -} + H^+ \rightarrow HO_2^\bullet$$

$$HO_2^\bullet + e^- \rightarrow HO_2^-$$

$$HO_2^- + H^+ \rightarrow H_2O_2$$

$$H_2O_2 + e^- \rightarrow OH^- + HO^\bullet$$

$$S + HO^\bullet \rightarrow CO_2 + H_2O$$

When the Bi:TiO_2 photocatalyst is radiated by visible light with a photon energy higher or equal to the band gap between the top of the (lone pair) Bi^{3+} 6s band and the bottom of the Ti^{4+} 3d band, electrons (e^-) in the 6s level of Bi^{3+} can be excited into the VB of TiO_2, leaving same amount of holes (h^+) in the 6s level of Bi^{3+}. Then holes are captured by surface hydroxyl groups (OH^-) at the photocatalyst surface to yield hydroxyl radicals ($HO^\bullet$) [19], and the electrons are trapped by the dissolved oxygen molecules (O_2), producing superoxide anions ($O_2^{\bullet -}$) [20]. The formed superoxide anions ($O_2^{\bullet -}$) may either attack the organic molecules directly or generate hydroxyl radicals ($HO^\bullet$) by reacting with hydrion (H^+) and photogenerated

electrons [21,22]. Afterward, hydroxyl radicals (HO•), as strong oxidizing agents, degrade the organic molecules [23].

4. Conclusion

Bi-doped TiO_2 nanofibers with variable Bi:Ti ratios have been successfully fabricated by an electrospinning method. Doping Bi species improved the separation of photogenerated electron and hole and extended the absorption of TiO_2 into visible light region due to the new energy states introduced by Bi, and 3% Bi:TiO_2 samples showed the highest photocatalytic activities. It is expected that such nanofibrous structures would provide great impetus to the industrialization of photocatalysts in the wastewater remediation.

Acknowledgement

We acknowledge the financial support from the National Natural Science Foundation of China (50972155, 50902144, 50732004), National Basic Research Program of China (2010CB933503) and the Nanotechnology Programs of Science and Technology Commission of Shanghai (0952nm00400).

Appendix A. Supplementary data

Supplementary data associated with this article can be found, in the online version, at doi:10.1016/j.jhazmat.2011.09.010.

References

[1] M.R. Hoffmann, S.T. Martin, W.Y. Choi, D.W. Bahnemann, Environmental applications of semiconductor photocatalysis, Chem. Rev. 95 (1995) 69–96.
[2] C.C. Chen, W.H. Ma, J.C. Zhao, Semiconductor-mediated photodegradation of pollutants under visible-light irradiation, Chem. Soc. Rev. 39 (2010) 4206–4219.
[3] X. Chen, S.S. Mao, Titanium dioxide nanomaterials: synthesis, properties, modifications, and applications, Chem. Rev. 107 (2007) 2891–2959.
[4] J. Choi, H. Park, M.R. Hoffmann, Effects of single metal-ion doping on the visible-light photoreactivity of TiO_2, J. Phys. Chem. C 114 (2010) 783–792.
[5] H.Y. Li, D.J. Wang, P. Wang, H.M. Fan, T.F. Xie, Synthesis and studies of the visible-light photocatalytic properties of near-monodisperse Bi-doped TiO_2 nanospheres, Chem. Eur. J. 15 (2009) 12521–12527.
[6] Y.Q. Wu, G.X. Lu, S.B. Li, The doping effect of Bi on TiO_2 for photocatalytic hydrogen generation and photodecolorization of Rhodamine B, J. Phys. Chem. C 113 (2009) 9950–9955.
[7] S. Sajjad, S.A.K. Leghari, F. Chen, J.L. Zhang, Bismuth-doped ordered mesoporous TiO_2: visible-light catalyst for simultaneous degradation of phenol and chromium, Chem. Eur. J. 16 (2010) 13795–13804.
[8] Z.F. Bian, J. Ren, J. Zhu, S.H. Wang, Y.F. Lu, H.X. Li, Self-assembly of $Bi_xTi_{1-x}O_2$ visible photocatalyst with core-shell structure and enhanced activity, Appl. Catal. B 89 (2009) 577–582.
[9] Y. Yang, C.C. Zhang, Y. Xu, H.Y. Wang, X. Li, C. Wang, Electrospun Er:TiO_2 nanofibrous films as efficient photocatalysts under solar simulated light, Mater. Lett. 64 (2010) 147–150.
[10] A. Greiner, J.H. Wendorff, Electrospinning: a fascinating method for the preparation of ultrathin fibres, Angew. Chem. Int. Ed. 46 (2007) 5670–5703.
[11] M. Shang, W.Z. Wang, J. Ren, S.M. Sun, L. Wang, L. Zhang, A practical visible-light-driven Bi2WO6 nanofibrous mat prepared by electrospinning, J. Mater. Chem. 19 (2009) 6213–6218.
[12] C.H. Wang, C.L. Shao, L.J. Wang, L. Zhang, X.H. Li, Y.C. Liu, Electrospinning preparation, characterization and photocatalytic properties of Bi_2O_3 nanofibers, J. Colloid Interface Sci. 333 (2009) 242–248.
[13] W.F. Yao, H. Wang, X.H. Xu, X.F. Cheng, J. Huang, S.X. Shang, X.N. Yang, M. Wang, Photocatalytic property of bismuth titanate $Bi_{12}TiO_{20}$ crystals, Appl. Catal. A 243 (2003) 185–190.
[14] H. Yamashita, Y. Ichihashi, S.G. Zhang, Y. Matsumura, Y. Souma, T. Tatsumi, M. Anpo, Photocatalytic decomposition of NO at 275 K on titanium oxide catalysts anchored within zeolite cavities and framework, Appl. Surf. Sci. 121 (1997) 305–309.
[15] B.S. Liu, X.J. Zhao, L.P. Wen, The structural and photoluminescence studies related to the surface of the TiO_2 sol prepared by wet chemical method, Mater. Sci. Eng. B 134 (2006) 27–31.
[16] T. Toyoda, T. Hayakawa, K. Abe, T. Shigenari, Q. Shen, Photoacoustic and photoluminescence characterization of highly porous, polycrystalline TiO_2 electrodes made by chemical synthesis, J. Lumin. (2000) 1237–1239, 87–9.
[17] S. Shamaila, A.K.L. Sajjad, F. Chen, J.L. Zhang, Study on highly visible light active Bi_2O_3 loaded ordered mesoporous titania, Appl. Catal. B 94 (2010) 272–280.
[18] H. Mizoguchi, K. Ueda, H. Kawazoe, H. Hosono, T. Omata, S. Fujitsu, New mixed-valence oxides of bismuth: Bi1 − *x*Y*x*O1.5 + delta (*x* = 0.4), J. Mater. Chem. 7 (1997) 943–946.
[19] N. Zhang, S.Q. Liu, X.Z. Fu, Y.J. Xu, Synthesis of M@TiO_2 (M = Au, Pd, Pt) core-shell nanoconnposites with tunable photoreactivity, J. Phys. Chem. C 115 (2011) 9136–9145.
[20] J. Yang, C.C. Chen, H.W. Ji, W.H. Ma, J.C. Zhao, Mechanism of TiO_2-assisted photocatalytic degradation of dyes under visible irradiation: photoelectrocatalytic study by TiO_2-film electrodes, J. Phys. Chem. B 109 (2005) 21900–21907.
[21] L.R. Zheng, Y.H. Zheng, C.Q. Chen, Y.Y. Zhan, X.Y. Lin, Q. Zheng, K.M. Wei, J.F. Zhu, Network structured SnO_2/ZnO heterojunction nanocatalyst with high photocatalytic activity, Inorg. Chem. 48 (2009) 1819–1825.
[22] H.C. Yatmaz, A. Akyol, M. Bayramoglu, Kinetics of the photocatalytic decolorization of an Azo reactive dye in aqueous ZnO suspensions, Ind. Eng. Chem. Res. 43 (2004) 6035–6039.
[23] O. Legrini, E. Oliveros, A.M. Braun, Photochemical processes for water-treatment, Chem. Rev. 93 (1993) 671–698.